PHYSICAL REVIEW B VOLUME 24, NUMBER 12 15 DECEMBER 1981

Simplified theory of dislocation damping including point-defect drag. I. Theory of drag by equidistant point defects

K. Lücke
Institut für Allgemeine Metallkunde und Metallphysik, Technische Hochschule, Aachen, Germany

A. V. Granato
*Physics Department and Materials Research Laboratory, University of Illinois at Urbana-Champaign, Urbana, Illinois 61801**
and Institut für Allgemeine Metallkunde und Metallphysik, Technische Hochschule, Aachen, Germany
(Received 22 June 1981)

The theory of dislocation damping for movable pinning points is developed by using results found earlier by the authors for the relaxation strength and relaxation time for the damped vibrating-string model. In this way new formulas are not needed but only a reinterpretation of the constants of the old theory. This is justified by exact calculations for the case of n equidistant movable pinners. It is shown that the results can be represented in good approximation in the form of Debye relaxations. Four different such approximations are considered and compared. It is found that the main dependence of the effects on the parameters for any number of movable pinning points is the same as that for a continuously dragged string with only small changes of the order of 30% or less in numerical factors for the relaxation time and strength. These changes are of the same order as those introduced by a Debye approximation. The relation of the results to earlier work is discussed. In addition, the theory is placed within the framework of an even more general theory formulated in terms of a rigid-rod approximation.

I. INTRODUCTION

In the past twenty years, the notion that point-defect drag by dislocations should give rise to internal-friction peaks has been suggested by numerous authors. Many theories for the process have been presented independently which are either for limiting assumptions or in a form which is so complex that it is difficult to discuss the dependence of the effect on the essential parameters. We believe that drag effects will prove to be ubiquitous and that a simplified but complete and realistic form of the theory will be not only useful, but necessary, for the confrontation of experiments with theory.

The purpose of the present series of three articles is (1) to present such a simplified theory, (2) to relate the previous theories to each other and to show them as part of a unified framework, (3) to show that in particular the theory of point-defect drag can be considered to be a limiting case of the previously existing damped vibrating-string theory, rather that vice versa as has been suggested, (4) to calculate the exact solution for the case of drag by equidistant pinners and to compare this with the above simplified theory, (5) to find a preferred approximation among the various possible Debye approximations for a vibrating string, (6) to place these results within the framework of an even more general theory—the rigid-rod approximation, (7) to consider the effects of superposition of different physical sources of restoring and viscous drag forces, (8) to consider the effects of distributions of pinning points, and (9) to discuss the dependence of the decrement and modulus on the different experimental parameters.

Points (1)—(6) are contained in the present paper (hereafter called paper I). Paper II contains (7) above and leads to a fuller understanding of the basic physics of drag effects. Paper III, to be pub-

lished in the near future, contains points (8) and (9) and leads to formulas more suitable for the evaluation of experimental data.

After giving a survey of the theoretical situation in the field, in paper I two limit cases are treated: It is assumed that the drag is either only of continuous or only of discrete nature, i.e., that it is acting on the full length of, or pointwise at, the dislocation (pinning-point drag). By using simple physical arguments it is shown that the damping due to movable pinning points can also be described well by the theory derived earlier by the authors for a damped vibrating-string model with continuous drag. In this way, new formulas are not needed, only a reinterpretation of the constants of the old Granato-Lücke formulas is necessary. By exact calculations it is shown that for both continuous and discrete drag the resulting phenomena can be described to a very good approximation as simple Debye relaxations. The deviations from this and their physical reasons are discussed.

In a second paper (paper II) the superposition of continuous and discrete drag [point (7)] is treated. Again, the main results are obtained by stressing physical arguments and simplified models and by using exact calculations mainly for checking the accuracy of the approximations. This leads to a fuller understanding of the basic physics of drag effects. In contrast to papers I and II where only equidistant pinning points are considered, distribution effects of pinning points will be taken into account in paper III. This leads to formulas more suitable for the evaluation of experimental data so that a useful discussion of the dependence of the resulting effects upon the experimental parameters can also be given [points (8) and (9) above].

II. DISCUSSION OF EARLIER WORK

In 1956, Granato and Lücke[1] derived a theory for damping and modulus changes due to dislocation motion, which was based on the vibrating-string model of Koehler.[2] In Koehler's model it is assumed that the dislocation is fixed at certain places by pinning points and that, under the influence of external periodic shear stresses, the free dislocation segments or loops between the pinning points undergo forced vibration. In the extension of this theory by Granato and Lücke two kinds of pinning points, strong and weak, are taken into account. These are characterized by the phenomenological parameters L_N and L_c, which describe the average distance L_N between strong (or firm) pinning points, and the average distance L_c between all pinning points. For sufficiently large stresses, the dislocation can overcome the retarding force of the weak pins, but not of the strong pins.

The inelastic nature of the response of the crystal to the external stress results from the assumption that the motion of the dislocations is opposed by a viscous force. A number of possibilities for the physical source of this drag have been discussed. These can be divided into two groups.

(i) The first group involves a drag acting continuously along the dislocation line. This has been assumed in the original Granato-Lücke theory and results in internal-friction phenomena which, in first approximation, can be described as a simple relaxation process. Many experimental observations have been explained on the basis of this "dislocation resonance theory." The interaction of dislocations with phonons and electrons and the losses due to sound irradiation by vibrating dislocations belong in this category. Under many circumstances the phonon drag mechanism[3] seems to be the main source of damping.[4,5]

(ii) The second group involves a drag action pointwise at the dislocation resulting from its interaction with point defects. Here several mechanisms have been treated, e.g., the breakaway of the dislocation from defects or the diffusion of the defects along or with the dislocation. The mechanism of principal interest for this paper is the latter one: The moving dislocation drags the pinning points with it without breaking away from them.

The process of point-defect drag as a mechanism for internal friction has been proposed by many authors. It seems to have been first mentioned by Kessler[6] (1957) and by Weertman[7] (1957), who suggested that high-temperature damping could be treated by applying the theory of Cottrell and Jaswon[8] for dragging of an extended Cottrell atmosphere. Kamel[9] (1961), without any calculations, tried to explain relaxation effects he observed in quenched gold by dragging of vacancies. Schoeck[10] (1962) proposed impurity drag as the source of an internal-friction peak observed after cold work in bcc metals and calculated the decrement under the assumption that the impurities that could be dragged provide a continuous viscous drag. The resulting expression for the decrement is that for an overdamped string with the time constant determined by the diffusivity of the impurities.

In these papers (although not always exactly

specified), the interaction of the dislocations with point defects was more or less treated as having a continuous nature, and the activation energy of damping was taken to be that of lattice diffusion. A calculation assuming the point defects to be situated directly at the dislocation core and acting pointwise at the dislocation (movable pinning points) was given by Schiller[11] (1964), but he allowed for only a single diffusion jump for the point defects in each direction. This is correct only for very high frequencies and otherwise leads to grave errors. Blistanov and Shaskolskaya[12] (1964) derived the decrement arising from the simultaneous action of pinning-point drag and of phonon drag, but only for a limited frequency range (below the phonon drag peak and above the point-defect drag peak). Bauer[13] (1965) noted that the diffusion of pinning points occurring near the dislocation core should be facilitated, but he was thinking only of diffusion parallel to the dislocation line and thus considered only the effects on the string model of the corresponding loop-length changes.

A rather general discussion of the problem of internal friction due to pinning-point diffusion was given by Lücke and Schlipf[14] (1968). In particular: (i) They included a discussion of perpendicular and parallel diffusion and of the distribution of pinning points under the influence of entropy forces. (ii) As special examples, they treated, among others, the cases of perpendicular diffusion of a single movable pinning point per dislocation loop and the case of many pinning points per loop, in the latter case reducing the problem to the continuous case. They found that these processes could be described in the form of Debye relaxation processes, and gave expressions for the relaxation strengths and relaxation times. (iii) They pointed out that, as with the parallel motion, the diffusion of such pinning points perpendicular to the dislocation line is also facilitated, since the dislocation immediately follows the motion of the pinning point by slip so that the pinning point always remains close to the dislocation core. In this way activation energies smaller than that for lattice diffusion could be explained. Work along this line was continued by Schlipf, Winkler-Gniewek, and Schindlmayr[15] (1973), who found that the process becomes amplitude dependent at high enough stress amplitudes.

Simpson and Sosin[16,17] (1972) published a series of papers in which the problem of internal-friction phenomena due to pinning-point dragging was treated again. Their work differed from previous treatments, mainly by (i) considering the simultaneous action of continuous and pinning-point-defect drag for all frequencies, (ii) considering additional special cases including some questions concerning loop-length distributions, (iii) assuming the drag mechanism to be athermal, while it was supposed in all previous treatments that the pinning points move by diffusion, and (iv) attempting to interpret irradiation-induced changes of internal friction by an increase of the number of dragged pinning points in frequency and temperature ranges, where in previous treatments (e.g., for copper in the kHz range at and below room temperature) changes in the number of firm pinning points had been mostly assumed.

More recently, Ogurtani[18] claims to have obtained the complete solution of dislocation damping for the equally spaced multidragging point-defect case, from which he finds that the Simpson-Sosin dragging model is equivalent to the damped vibrating-string model. However, his solution appears to be that for a continuously distributed drag, and does not display the existence of a second component to the response which is shown in paper II to be an essential feature of a complete solution for drag produced by discrete point defects. For the continuous drag case, the equivalence of the models is self-evident.

Although the considerations of Simpson and Sosin were independent of some of the earlier work, the model that they refer to as the SS model is exactly the same and their results are in quantitative agreement with those given earlier.[14] Also, it has been claimed[17] that the dragging model is a more general formulation of the dislocation damping problem with the damped vibrating-string model as its high-frequency limit. We will follow here the opposite viewpoint, according to which the defect dragging model is a special case of the damped vibrating-string model. The advantage of the latter viewpoint is that the old string theory can be used as is by simply reinterpreting the constants of the theory. This also emphasizes the underlying unity of the subject.

The damped string model theory given earlier by the writers is not limited to phonon drag and fixed pinning points, as implied by Simpson and Sosin. It is a phenomenological theory, with no specific mechanism specified for the viscous drag. Different mechanisms have been considered before, requiring only a reinterpretation of the parameters. For example, at high temperatures the phonon drag dominates in many cases; at low temperatures

the electron drag takes over in metals[4,5]; in superconductors at low temperatures, the electron drag goes to zero, but a radiation drag remains, which can be taken into account by allowing the drag constant to be frequency dependent.[19] Other frequency-dependent drag constants have also been considered,[20] and kink motion has been taken into account by reinterpreting dislocation-line tensions in terms of kink densities.[21,22] As mentioned earlier, the dragging of point-defect atmospheres has also been included in this scheme. In Secs. III and IV of this paper it will be shown that in a good approximation this description even holds for a pointwise-acting pinning-point drag.

The solutions given by Simpson and Sosin for the combined action of continuous and pinning-point drag are very general, but are complicated mathematically and difficult to discuss. They have therefore only been applied to the limit cases already known before, namely that either only continuous or point-defect drag is effective and, in the latter case, only for simple situations. Therefore, in paper II another treatment is given which is again based on simple physical arguments and the old Granato-Lücke theory. The greater transparency of this treatment makes it possible to discuss more clearly the influence of different parameters and also to discuss parameters not considered by Simpson and Sosin.

III. SIMPLIFIED DESCRIPTION OF CONTINUOUS AND DISCRETE DRAG BY THE GRANATO-LÜCKE FORMULAS

The basic process considered in the Granato-Lücke theory of dislocation resonance is the forced vibration of a dislocation segment of length L_N firmly and unbreakably fixed at its ends under exposure to a periodic external stress $\sigma=\sigma_0 e^{i\omega t}$ (Fig. 1). The dislocation displacement $y(x,t)$ is a solution of Koehler's equation of motion:

$$A\frac{\partial^2 y}{\partial t^2}+B\frac{\partial y}{\partial t}-C\frac{\partial^2 y}{\partial x^2}=b\sigma_0 e^{i\omega t}\,. \tag{1}$$

A is the dislocation mass per unit length, B is a viscous drag constant, and C is the dislocation-line tension. With solutions in the form $y(x,t)=\eta(x)e^{i\omega t}$, where η is the (complex) displacement amplitude, the modulus defect $\phi=\Delta M/M$ and damping δ are then given by the real ($\bar{\eta}_R$) and imaginary ($\bar{\eta}_I$) components of the average displacement amplitude $\bar{\eta}$ as

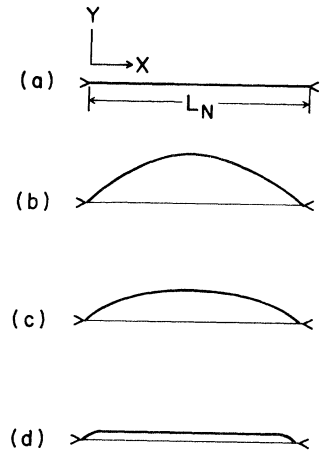

FIG. 1. Displacement y vs x for continuous drag on a dislocation of length L_N. (a) No stress applied. (b) Displacement at low frequency. (c) Displacement at intermediate frequency. (d) Displacement at high frequency.

$$\phi=\frac{\Delta M}{M}=\frac{Gb\Lambda}{\sigma_0}\bar{\eta}_R\,,\quad \delta=Q^{-1}=\frac{\Delta}{\pi}=\frac{Gb\Lambda}{\sigma_0}\bar{\eta}_I\,, \tag{2}$$

where G is the shear modulus, b is the Burgers vector, and Λ is the total dislocation length per unit volume. (To reduce the number of superscripts and letters the symbol δ is used here instead of Q^{-1}, ϕ instead of $\Delta M/M$, and Δ instead of Δ_R for the relaxation strength.) In Eq. (2) an orientation factor Ω giving the resolved shear stress on the slip planes for a given external stress should appear, but has been set equal to unity, as this factor will not be considered here.

In all that follows, the drag B will be assumed to be large enough so that the dislocations are overdamped. Then, according to the above theory, such dislocation motion causes damping and modulus changes whose frequencies dependence is described to a very good approximation by a simple Debye relaxation process. This means that ϕ and δ have the form

$$\phi=\Delta\frac{1}{1+(\omega\tau)^2}\,,\quad \delta=\Delta\frac{\omega\tau}{1+(\omega\tau)^2} \tag{3}$$

with

$$\omega_m=\frac{1}{\tau}\quad\text{and}\quad \delta_m=\frac{\Delta}{2} \tag{4}$$

as the frequency and magnitude of the damping at its maximum value. The relaxation strength Δ and

the relaxation time τ are given as

$$\Delta=\frac{1}{\kappa}\frac{Gb^2}{12C}\Lambda L^2\ ,\quad \tau=\frac{1}{\gamma}\frac{BL^2}{12C} \tag{5}$$

with

$$\kappa=\frac{\pi^4}{96}=1.015\approx 1\ ,\quad \gamma=\frac{\pi^2}{12}=0.822\approx 1\ . \tag{6}$$

(These factors κ and γ differ from those introduced in Ref. 22 as discussed in Sec. V.)

Equations (3)—(6) are approximate relations, corresponding to the first term of a Fourier series expansion of η. Exact solutions can also be given, but these are in general much more complicated expressions which are only slightly more accurate than those given above. Furthermore, the form of the exact solutions obscures the important physical fact that the process is basically of a simple relaxation form. Small deviations from the simple behavior given by Eqs. (3)—(6) will be discussed in the following section. In fact, none of these have been detected experimentally so far in investigations of strongly overdamped dislocation motion.

The drag force B may have many sources. Two models for the type of B will be considered here.

The first is the old continuous Granato-Lücke model. It is assumed that the dislocations are divided into network segments of length L_N with firmly fixed ends [Fig. 1(a)] and that the drag is of a continuous nature. Combining the different continuously acting drag sources, e.g., phonons ($B_{\rm ph}$), electrons ($B_{\rm el}$) or re-radiation ($B_{\rm rr}$), into a single continuous drag called $B_c=B_{\rm ph}+B_{\rm el}+B_{\rm rr}+\cdots$, one obtains the relaxation strength Δ_N and relaxation time τ_N directly from Eq. (5) and (6) by using $L=L_N$ and $B=B_c$:

$$\Delta_N=\frac{1}{\kappa}\frac{Gb^2}{12C}\Lambda L_N^2\ ,\quad \tau_N=\frac{B_cL_N^2}{12\gamma C}\ . \tag{7}$$

In a second model it is assumed that the continuous drag is zero, but movable pinning points act on the dislocation at discrete places. Thus it is assumed that each network length L_N contains $p=(n-1)$, where $n=L_N/L_d$, equidistant movable pinning points [Fig. 2(a)], each of which has the mobility m. [The length in earlier work[1] called L_c (c standing for concentration) will now be denoted by L_d, indicating the discrete nature of point-defect drag. The subscript c (e.g., in B_c) will be used to characterize continuous drag effects.] Related to an infinite dislocation, this leads to an

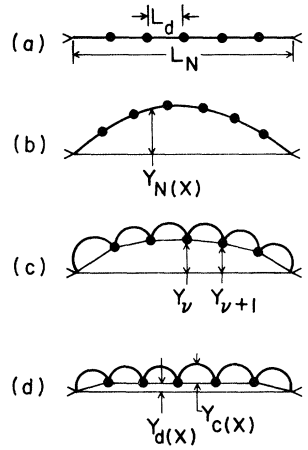

FIG. 2. Displacement y vs x for discrete drag by pinning points at x_ν spaced a distance L_d apart. (a) No stress applied. (b) Displacement at low frequency. (c) Displacement at intermediate frequency. (d) Displacement at high frequency.

average drag constant for discrete drag of

$$B_d=\frac{1}{mL_d}=\frac{n}{mL_N}\quad\text{with } m=\frac{D}{kT}\ , \tag{8}$$

where D is the diffusivity of the movable pinning points.

It can easily be recognized that such a pointwise concentration of drag simply corresponds to the well-known textbook topic of replacing a continuous string by a linear chain of mass points (except that here the emphasis is on the frictional instead of on the usually considered inertial features). This insight allows one to conclude immediately that, from the qualitative-physical point of view, there is no basic difference in the vibration behavior of both models so that the general predictions of the string model (concerning the resonance and damping behavior) remain unchanged. Thus Eqs. (5) and (6) should give an approximation of the damping behavior in the case of pinning if one sets $L=L_N$ and $B=B_d$; i.e., it is

$$\Delta_d=\frac{1}{\kappa}\frac{\sigma b^2}{12C}\Lambda L_N^2\ ,\quad \tau_d=\frac{B_dL_N^2}{12\gamma C}\ . \tag{9}$$

For large enough numbers of participating "mass points," i.e., for $p>>1$, Eq. (9) is also quantitatively correct, and it should be a reasonable approximation even for values of p comparable to one.

Thus the results for point-defect drag are directly obtained from the Granato-Lücke formulas derived for continuous drag without further calculations. They correctly describe the basic physics

of this process and are quantitative approximations, as are the Granato-Lücke formulas themselves. There is, however, also a basic difference between the continuous and discrete case. In the discrete case one has in reality a superposition of two processes and thus two terms in the dislocation displacement: $y = y_d + y_c$. The displacement of the dislocation due to the motion of the pinning points is y_d and is given in Fig. 2 by the polygon. y_c is the superimposed displacement of the in-between loops. y_d is drag controlled, and thus is responsible for the relaxation effects. In the present case of $B_c = 0$, y_c is always in phase with the applied stress and does not depend upon the displacement of the pinning points (i.e., on y_d) or on frequency. It thus contributes only a frequency-independent modulus defect and can be forgotten for the relaxation effects considered in the present paper. (This does not hold for the case where $B_c \neq 0$, as will be shown in paper II.) With growing n, this modulus defect decreases and disappears completely for the continuous case $n = \infty$.

To provide a better understanding of the physical meaning of these effects the vibrations of the dislocations are illustrated in Figs. 1 and 2 schematically. Figure 1 represents the case of continuous drag. At very low frequencies [Fig. 1(b)] the displacement is essentially controlled by the restoring force and thus is parabola shaped and practically in phase with the external stress. At medium frequencies [Fig. 1(c)] a phase lag builds up, and at high frequencies [Fig. 1(d)] where the motion is essentially drag controlled, the phase lag is nearly 90°. In this case all points of the dislocation except near the ends have the same displacement (rigid-bar-type motion). One recognizes that at low frequencies the displacement is nearly completely in phase with the stress and mainly contributes to the modulus defect, whereas at high frequencies where it is nearly completely out of phase, it contributes practically only to the damping. Thus the low-frequency modulus defect and high-frequency damping are zero-order effects since, in these frequency ranges, the other property represents only a correction to the displacement.

In the case of pure point-defect drag (Fig. 2), the continuous drag at the dislocation segments L_d is zero so that these will be able to follow the external force without delay, i.e., they will always be parabola shaped and will transmit the external driving force to the pinning points exactly in phase with the applied stress. At low enough frequencies [Fig. 2(b)], the pinning points are also able to follow the dislocation motion without delay. This means their displacements $y_d(t)$ are nearly in phase with the stress and given by the same parabola that would be formed by the dislocation without pinning points [Fig. 1(b)]. At medium frequencies [Fig. 2(c)], the pinning points move, but with an amplitude smaller than that of a free dislocation and with a phase lag. At very large frequencies [Fig. 2(d)], finally, one has mainly the vibration of the in between (L_d) dislocation segments and only very little motion of the pinning points. Since the pinning point motion is mainly drag controlled, the displacements $y_d(t)$ of the different pinning points are nearly 90° out of phase and are all of the same size (rigid-bar-type motion).

IV. QUANTITATIVE DESCRIPTION OF CONTINUOUS AND DISCRETE DRAG

In the preceding section, dislocation motion exposed to a continuous or discrete drag has been described by expressions corresponding to a Debye-type relaxation [Eqs. (3)–(9)]. This description is only approximately correct. An exact description had been given for the continuous case by Granato and Lücke[1] in the form of an infinite Fourier series. It follows from the solution of the equation of motion (1) and is given (for the mass $A = 0$) in Appendix A. The case of point-defect drag has so far been discussed in the literature only numerically.[16] In Appendix C an exact analytical description not previously presented (again for $A = 0$) is derived in the form of a finite Fourier series. It is obtained by solving a set of difference equations, which replaces the differential equation (1) and represents the equations of motion of the movable pinning points under the influence of the line tension of the dislocation loops L_d.

These exact expressions, however, are difficult to discuss, and, as will be shown, differ in only minor respects from the above Debye-type expressions. It is therefore useful to approximate the exact solution with a Debye form. This can be done in several ways. We consider four different such approximations, each of which gives a fair overall approximation for the correct expression while approximating especially well certain features of it. (These are illustrated for the continuous case in Fig. 3.)

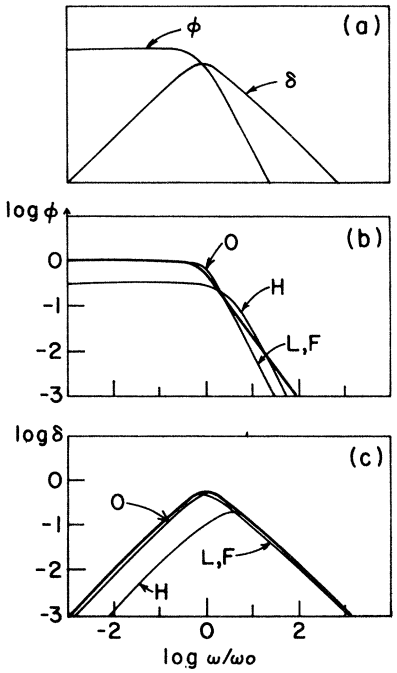

FIG. 3. Schematic illustration of four Debye approximations to the decrement and modulus of a dislocation with continuous drag. (a) Exact modulus and decrement versus log frequency. (b) Fits of Fourier (F), low-frequency (L), high-frequency (H), and zero-order (O) approximations to the modulus. (c) Same fits to the decrement.

(1) The low-frequency approximation is obtained by fitting a Debye form accurately to the decrement and modulus at low frequencies.

(2) A high-frequency approximation is obtained by fitting accurately the decrement and modulus at high frequencies.

(3) Fourier approximation— by using the first term of a Fourier expansion an approximation is obtained which is rather similar to the low-frequency approximation but gives a somewhat better overall description, especially near the maximum of the decrement.

(4) The zero-order approximation is obtained by fitting accurately the modulus at low frequency and the decrement of high frequencies. Although this is "mixed" in the sense of not being best fitted for both modulus and decrement in a definite frequency range, the approximation has a number of advantages.

(i) It is a natural approximation in the sense that the first-order effects at low and high frequency are the modulus and decrement, respectively.

(ii) As described in Appendix B, the approximation can be obtained without solving the full differential equations [Eq. (1)]; only a simpler differential equation need be solved. This makes it possible to solve problems in this approximation which are intractable in other approximations, for example, many questions concerning distributions of pinning points (paper III).

(iii) The zero-order approximation is closely related to a more general formulation, the rigid-rod approximation, described in Sec. V. In the rigid-rod approximation, no differential equation need be solved at all, but a certain kind of useful Debye fit is obtained again by considering the modulus at low frequency and the decrement at high frequency.

For all these reasons, the zero-order approximation becomes preferred over the others.

These four different approximations are considered in detail for the continuous case in Appendix A and for the discrete case in Appendix C. It is found that for all approximations, the dependences upon the main parameters and thus Eqs. (5) and (9) for Δ and τ are retained and that only the numerical factors κ and γ differ from those given by Eq. (6). Thus it is possible to describe rather completely but simply the internal friction due to continuous and point-defect drag by giving the κ and γ values corresponding to different n and different approximations. For this reason these factors have been calculated and listed in Table I as a function of n including the continuous case with $n=\infty$. The subscripts L, H, F, and 0 are used to represent the value of κ and γ for given n of the low, high, Fourier, and zero-order approximations, respectively. The fact that for a given value of n, κ and γ differ for different approximations indicates that there are deviations from the exact Debye-type frequency dependence, Eq. (3). These, however, are rather small ($<33\%$). Similar differences occur if n is changed from 2 to ∞. Some of these differences in the κ and γ values of Table I can be predicted without further calculations.

(1) For $n=2$ and 3 there is only a single even mode and, correspondingly, an exact Debye-type frequency dependence. This shows itself in the fact that κ and γ are the same for all approximations.

(2) The change of $\kappa_L(n)$ is rather simple to understand. Here at low frequencies the pinning displacement is in phase with the stress and thus the area swept out by the corresponding dislocation gives the modulus defect ϕ. Since, in this frequen-

TABLE I. κ and γ factors for relaxation strengths and relaxation times defined by $\Delta=[(Gb^2 12C)\Lambda L^2]/\kappa$ and $\tau=[BL^2/12C]/\gamma$. The factors depend upon the Debye-type approximation used, indicated by a subscript, and the number $n-1$ of dragged point defects in a dislocation segment L. The first row (n) gives values for the general case while the last line ($n=\infty$) gives values for continuously distributed drag.

Approximation n	$\kappa_0(n)$	Zero order $\gamma_0(n)$	$\gamma_0(n)/\kappa_0(n)$	$\kappa_L(n)$	Low frequency $\gamma_L(n)$	$\gamma_L(n)/\kappa_L(n)$	First-term Fourier[a] $\kappa_F(n)$	$\gamma_F(n)$	$\gamma_F(n)/\kappa_F(n)$	High frequency[b] $\kappa_H(n)$	$\gamma_H(n)$	$\gamma_H(n)/K_H(n)$
n	$\frac{1}{1-1/n^2}$	$\frac{1}{1+1/n}$	$1-1/n$	$\frac{1}{1-1/n^2}$	$\frac{5/6}{1+1/n^2}$	$\frac{5(1-1/n^2)}{6(1+1/n^2)}$	$\frac{n^3}{b_1^{(n)}}\frac{\sin^2(\pi/2n)}{\cot(\pi/2n)}$	$\frac{n^2}{3}\sin^2\frac{\pi}{2n}$	$\frac{b_1^{(n)}}{n}\cot\frac{\pi}{2n}$	$\frac{n^3}{6(n-1)^2}$	$\frac{n^2}{6(n-1)}$	$1-1n$
2	1.3333	0.6667	0.5	1.3333	0.6677	0.5	1.3333	0.6667	0.5	1.3333	0.0667	0.5
3	1.125	0.75	0.6667	1.125	0.75	0.6667	1.125	0.75	0.6667	1.125	0.75	0.6667
4	1.0667	0.8	0.75	1.0667	0.7843	0.7353	1.0727	0.7813	0.7283	1.1852	0.8889	0.75
$n\gg1$	$1+1/n^2$	$1-1/n$	$1-1/n$	$1+1/n^2$	$0.833(1-1/n^2)$	$0.833(1-2/n^2)$	$1.0147\left(1+\frac{1}{n^2}\right)$	$0.822\left(1-\frac{0.822}{n^2}\right)$	$0.806\left(1-\frac{0.822}{n^2}\right)$	$(n/6)(1+2/n)$	$(n/6)(1+1/n)$	$1-1/n$
∞	1	1	1	1	0.8333	0.8333	1.0147	0.8225	0.8106	$1.0147\frac{\sqrt{\omega\tau_0}}{2}$	$1.0147\frac{\sqrt{\omega\tau_0}}{2}$	1

[a]The coefficients $b_1^{(n)}$ are given by Eq. (C8).

[b]For the high-frequency approximation, the $n>>1$ row applies for $n^2<\omega BL^2/C$, while the $n=\infty$ row applies for $n^2>\omega BL^2/C$.

cy range, $\phi\propto 1/\kappa$ [Eqs. (2)–(5)], $1/\kappa$ is proportional to this area which, for $n=\infty$, is parabola shaped. For finite n, however, the area given by the polygon formed by the pinning points must be used [Fig. 2(c)]. [The additional area included by the L_c loops is a constant independent of frequency and thus does not contribute to the relaxation peak under consideration (compare paper II).] This is obtained by deducting the parabolic displacement of the L_d loops from the (parabolic) displacement of the L_N loop. Since the average displacement of the parabola-shaped dislocation is proportional to L^2, one obtains

$$\frac{1}{\kappa_L(n)}\propto(L_N^2-L_d^2)=L_N^2\left[1-\frac{1}{n^2}\right], \tag{10}$$

in agreement with Table I for both κ_L and κ_0.

(3) The change of γ/κ with n at high frequencies is also simple to understand. Here the pinning point displacement is nearly 90° out of phase and the area swept out by the corresponding dislocation displacement gives the damping δ. Since, in this frequency range, $\delta\propto\gamma/\kappa$ [Eqs. (2)–(5)], γ/κ is proportional to this area. For $n=\infty$, this area is rectangle shaped [Fig. 1(d)]. For finite n, however, deviations from the rectangle occur [Fig. 2(d)], and the area to be used is thus obtained by deducting that of the two triangles at the first and last L_d loop from the rectangle. Since their area corresponds to the fraction L_d/L_N of the rectangular area, one obtains

$$\frac{\gamma}{\kappa}\propto 1-\frac{L_d}{L_N}=1-\frac{1}{n}, \tag{11}$$

in agreement with Table I for both γ_H/κ_H and γ_0/κ_0.

So far, the n dependences of κ_L, κ_0, γ_H/κ_H, and γ_0/κ_0 are accounted for. These are zero-order effects. A physical discussion of the remaining κ's and γ's, which depend on second-order effects, is more difficult but still possible.

(4) The reason γ_F/κ_F differs from γ_H/κ_H is simply that the higher-order terms in a Fourier expansion are neglected for γ_F/κ_F. For large n these terms increase the damping by a factor $\pi^2/8$, accounting for the difference. γ_L/κ_L differs only slightly from γ_F/κ_F, and this difference can be understood in the same way.

(5) It is especially interesting to understand the dependence of κ and γ on frequencies in the high-frequency approximation for $n=\infty$. This arises from the fact that the modulus defect is not

described well at high frequencies by a Debye form, but shows a $(\omega\gamma)^{-3/2}$ instead of an $(\omega\gamma)^{-2}$ behavior. This can be understood simply with the help of Fig. 4. Each Fourier component to the displacement contributes a term to the modulus of Debye form with ω^{-2} dependence at high frequencies as given in Eq. (A4). For a frequency $\omega^* >> \omega_0$, all modes of frequency $\omega_j < \omega^*$ make equal contributions to ϕ, as seen in Fig. 4. The sum of the contributions in the region falls with $(\omega\gamma)^{-3/2}$, i.e., more slowly than $(\omega\gamma)^{-2}$. Nonetheless, the n and frequency dependence of κ and γ in the region can be understood easily and is discussed in Appendix C.

V. THE RIGID-ROD MODEL

In the foregoing sections it has been shown that the damping due to movable pinning points can be considered as a special case of the original vibrating-string model and that it can be described by the old Granato-Lücke formulas with slight changes of the factors γ and κ. In this section a further simplification and, at the same time, generalization of the dislocation resonance theory will be given. It mainly concerns the restoring force. The treatment is based on the rigid-rod model of dislocation motion which has recently been discussed by Lenz and Lücke[23] and Granato.[24]

In this model the dislocation is assumed to be straight and to have a displacement that is constant along its whole length [Fig. 5(a)]. Then, instead of Eq. (1) the equation of motion reads

$$B\dot{y}+Ky=b\sigma=b\sigma_0 e^{i\omega t} . \tag{12}$$

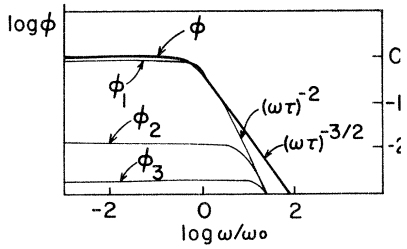

FIG. 4. Contributions to the dislocation modulus change for continuous drag as a function of frequency on a log-log scale. For a frequency $\omega^* >> \omega_0$, all modes of frequency $\omega j < \omega^*$ make equal contributions to ϕ, so that the frequency dependence is changed from $(\omega\tau)^{-2}$ to $(\omega\tau)^{-3/2}$ in the high-frequency range where the total modulus change is small.

Here Ky is the restoring force per unit length and K is a force constant. As can easily be found (and as is shown in paper II), this equation leads to a pure Debye-type relaxation with relaxation strength and relaxation time given by

$$\Delta=\frac{\Lambda Gb^2}{K} , \quad \tau=\frac{B}{K} . \tag{13}$$

In Eqs. (13), K and B are assumed to act continuously. It will now be shown that Eqs. (13) can also be applied if these quantities are of discrete nature, i.e., if the restoring force is supplied by firm pinning points [vibrating string, Fig. 5(b)] and/or the drag force by mobile pinning points [point-defect drag, Fig. 5(c)]. In these cases the quantities K and B must only be replaced by properly chosen effective quantities K_{eff} and B_{eff}.

The most natural way to obtain these effective quantities is to consider an infinitely long dislocation under constant stress σ. For the case of discrete restoring force [Fig. 5(b)], one may set the drag term in Eq. (12) to zero ($B=0$) and calculate the mean displacement of an dislocation loop of the length L_N. According to Appendix A one has $\langle y\rangle = b\sigma L_N^2/12C$ and obtains with $y=\langle y\rangle$

$$K_N=\frac{b\sigma}{\langle y\rangle}=\frac{12C}{L_N^2} . \tag{14}$$

For the case of discrete dragging force with mobile pinning points separated from each other by the distance L_d [Fig. 3(c)], one may set the restoring term in Eq. (12) to zero and obtain

$$B_d=\frac{b\sigma}{\dot{y}}=\frac{1}{mL_d} \tag{15}$$

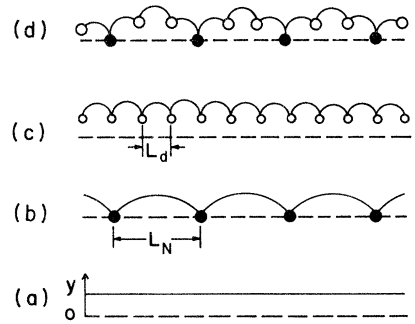

FIG. 5. Dislocation displacement under stress for different applied forces. (a) Continuous restoring and viscous forces (rigid rod). (b) Discrete restoring forces from fixed pinning points. (c) Discrete viscous forces from dragable pinning points. (d) Discrete restoring and viscous forces.

using $\langle \dot{y} \rangle = \dot{y}$ in agreement with Eq. (8).

Now let us consider the case where both restoring and pinning forces are discrete, i.e., a vibrating string with point-defect drag [Fig. 3(d)]. If one then would replace K and B by K_N and B in Eq. (13), one would recover the Granato-Lücke formula equation (4) except for the numerical factors κ and γ. This means, that, although the average restoring and dragging forces are taken into account correctly by Eqs. (14) and (15), some differences are still left between rod motion and string motion which reveal themselves in these factors. Thus, if one choses the effective quantities

$$K_{\text{eff}} = \kappa K_N \ , \quad B_{\text{eff}} = \beta B_d \tag{16}$$

to replace K and B in Eqs. (13), a complete agreement with Eq. (5) is obtained where $\gamma = \kappa/\beta$.

This all shows that all the dependencies upon the essential parameters for the considered model (here a vibrating string with point-defect drag) can be predicted without solving the general differential equation with its boundary conditions for this case [Eq. (1)]. Instead, the expressions for K_N and B_d, which according to Eqs. (14) and (15) can be found rather simply, have to be introduced into the rod equations (13). However, the exact values of the numerical factors κ and γ cannot be derived from the rigid-rod model but must be found by treating the considered geometry directly. These factors, however, are close to unity, as has been shown in Sec. IV and as can be seen in Table I. This means that a good approximate description of damping and modulus would be obtained even by neglecting these factors completely.

According to the above it follows from the rigid-rod equations that $\kappa = \gamma = 1$ if the correct average values K_N and B_d as given by Eqs. (14) and (15) are used. According to Table I the same values $\kappa = \gamma = 1$ are obtained for the zero-order approximation. This is because for this approximation, κ is determined by fitting the low-frequency modulus, i.e., by also using only the first term of Eq. (12) and by fitting the high-frequency damping, i.e., by using only the second term. Thus the zero-order approximation resembles the rigid-rod approximation.

VI. SUMMARY AND DISCUSSION

Summarizing the results of this paper, it is shown that the old Granato-Lücke-type equation (9) gives a good approximation for the description of damping and modulus defect not only for the case of continuous drag but also for the case of drag caused by movable point defects. The cases for various pinning-point numbers (including the continuous case $n = \infty$) and for various ways of approximating the exact solution by a Debye form differ only in the values of the numerical parameters κ and γ of the equation. These parameters are closely related to those introduced earlier by Lenz and Lücke[23] in a similar form of writing the general relations. They are found to change with frequency up to 20% (leading to a broadening of the Debye-type damping peak) and by a similar amount as n is changed from 2 to ∞. This means that this is the range of validity of this simplified theory. However, these small variations, i.e., the frequency and n dependence found in Table I, can be understood in simple physical terms.

Thus, by listing these parameters (Table I) a complete and extremely simple description of the different cases of drag by equidistant pinning points could be given. Also, the question about the meaning of the different values κ and γ, about which a certain confusion existed in the literature (e.g., the question of which is the "correct" value), has been clarified in this way. The more practical question of which values of κ and γ should be used in Eq. (9) is deferred until paper III, in which also the statistics of the pinning-point distribution is considered.

Furthermore, it has been shown that the expressions for the relaxation strength and time, Eqs. (13), can also be obtained by reference to the results for the rigid-rod model for continuous restoring and continuous drag. The quantities K and B have simply to be replaced by the quantities K_N and B_d. These are obtained by keeping one of the two quantities continuous and averaging the other one along the whole (infinite) dislocation line for constant stress [Eqs. (14) and (15)]. The results for the relaxation strength and relaxation time differ from the exact calculations only by the factors κ and γ given in Table I, i.e., factors of the order of 1.

This agreement suggests a further simplification and generalization. There is no question that under the influence of periodic external stresses the dislocations will vibrate, but often it will not be exactly clear what the exact geometry of the vibration is and what types of restoring and driving forces are acting. Then, according to the above, the rigid-rod equations can simply be used to obtain approximate numerical values for these quan-

tities from the measurements. Furthermore, if the types of restoring and drag forces are known, *approximate analytical* results can be obtained again without integrating the correct equation of motion. Only the averaged quantities K_i and B_i (the ones corresponding to K_N and B_d) must be found by the procedure corresponding to that in Eqs. (14) and (15) and must be introduced into Eq. (13) for K and B. In order to get a *correct* description of a given case, instead of K_i and B_i the effective quantities $K_{\text{eff}}=\kappa_i K_i$ and $B_{\text{eff}}=\beta_i B_i$ would have to be introduced. However, these numerical factors κ_i and β_i can again be expected to be ≈ 1.

In this way it seems to be possible to reduce all possible dislocation vibration geometries to the rigid-rod case, which leads to an exact Debye-type behavior. The deviations from the rigid-rod behavior due to the different geometries of other modes of vibrations or due to a non-Debye response can be accounted for by factors of the order of 1. The error introduced by this simplification (i.e., by these factors) will be smaller than the accuracy with which the other parameters entering these equations are known.

ACKNOWLEDGMENTS

This work was begun while one of the authors (A.V.G.) was in Aachen and completed in Urbana. A.V.G. is indebted to the Alexander von Humboldt Stiftung for an award which made the visit in Aachen possible. The work in Urbana is supported by the National Science Foundation under Grant No. NSF DMR80-15707.

APPENDIX A: RELAXATION EFFECTS CAUSED BY CONTINUOUS DRAGGING

In the following, the differences between the exact solution for the continuous case and the different Debye-type approximations listed in Sec. IV will be discussed. For this purpose the trial solution $y(x,t)=\eta(x)\exp(i\omega t)$ is introduced into Eq. (1). With $A=0$ it transforms Eq. (1) into the ordinary differential equation

$$i\omega B\eta - C\eta'' = \sigma_0 b \tag{A1}$$

with the boundary conditions $\eta(0)=\eta(L)=0$.

Exact solution. The exact solution of Eq. (1) was given in the form of a infinite Fourier series by Granato and Lücke.[1] For $A=0$ one obtains

$$\eta(x)=\sum_{\mu=0}^{\infty} a_{2\mu+1}\sin\frac{(2\mu+1)\pi x}{L_N} . \tag{A2}$$

Determining the coefficients $a_{2\mu+1}$ by inserting Eq. (A2) into Eq. (A1) and forming

$$\bar{\eta}=\frac{1}{L_N}\int_0^{L_N}\eta(x)dx = \sum_{\mu=0}^{\infty}\frac{2}{(2\mu+1)\pi}a_{2\mu+1} , \tag{A3}$$

one obtains for the real and imaginary parts

$$\bar{\eta}_R=\frac{8}{\pi^4}\frac{L_N^2}{C}b\sigma_0\sum_{\mu=0}^{\infty}\frac{1}{(2\mu+1)^4} \times\frac{1}{[1+(\omega\tau_F)^2/(2\mu+1)^4]} , \tag{A4}$$

$$\bar{\eta}_I=\frac{8}{\pi^4}\frac{L_N^2}{C}b\sigma_0\sum_{\mu=0}^{\infty}\frac{1}{(2\mu+1)^4} \times\frac{[\omega\tau/(2\mu+1)^2]}{[1+(\omega\tau_F)^2/(2\mu+1)^4]} .$$

Here $\tau_F=BL^2/\pi^2C$ is the relaxation time for the first Fourier component. Because of the neglect of the inertial term A, the possibilities of resonance at the frequencies $\omega=(2\mu+1)\omega_0$, where $\omega_0=(\pi/L_N)\sqrt{C/A}$, are suppressed in the above. This is a good approximation for $B>\sqrt{AC}/2L_N$. Also, even for the overdamped case, the inertial term would have led to a reduction in the decrement δ at high frequencies as $1/\omega^3$ instead of the $1/\omega$ given by Eq. (A4). This frequency range, however, lies above ω_0 and is normally not reached. Now the four approximations mentioned in Sec. IV will be applied.

(1) First-term Fourier approximation ($\kappa=\kappa_F$, $\gamma=\gamma_F$). Using only the first term of the Fourier expansion in Eq. (A4) leads to the values of κ_F and γ_F of Eq. (6). This is a good overall approximation, especially near the damping maximum. This is shown by the fact that to describe the height and the frequency of the damping maximum following from the exact solution, the values $\kappa=1.012$ and $\gamma=0.825$ must be used in Eq. (5). These differ from those of Eq. (6) by $<0.3\%$.

(2) Low-frequency approximation ($\kappa=\kappa_L$, $\gamma=\gamma_L$). This approximation follows directly from the exact solution equation (A4) by neglecting the terms $\omega^2\tau_F^2$ with respect to one. Since $\sum_{\mu=0}^{\infty}1/(2\mu+1)^k=\pi^4/96$ and $\pi^6/960$ for

$k=4$ and 6, one then obtains from Eqs. (A4) and (10) the values $\kappa_L=1$ and $\gamma_L=\frac{5}{6}$ for Δ and τ. This is more accurate in describing the response at low frequencies than that given by the values in Eq. (6), but the deviations are small ($<1.5\%$) and originate in the fact that for low frequencies the displacement of the dislocation is better described by parabolas than by the first Fourier term sine function of Eq. (A2).

For comparison purposes it is useful to derive these values of κ and γ directly from the differential equation (A1). For low frequencies, the first term of Eq. (A1) becomes small with respect to the others and can be considered as a perturbation. Thus, with a perturbation-type trial solution $\eta=\eta_{(0)}+\eta_{(1)}+\cdots$, one obtains

$$C\eta''_{(0)}=-b\sigma_0\,,$$
$$C\eta''_{(1)}=i\omega B\eta_{(0)}\,. \tag{A5}$$

Solving these equations for the above boundary conditions leads to

$$\eta_{(0)}=\frac{b\sigma_0}{2C}x(L_N-x)\,, \tag{A6}$$
$$\eta_{(1)}=\frac{iC\omega Bb\sigma_0}{24C^2}[L_N^2x(L_N-x)+x^2(L_N-x)^2]\,,$$

and

$$\bar{\eta}_{(0)}=b\sigma_0L_N^2/12C\,, \tag{A7}$$
$$\bar{\eta}_{(0)}=i\omega\beta b\sigma_0L_N/120C\,.$$

Equations (A7) with Eq. (2) yield $\kappa_L=1$ and $\gamma_L=\frac{5}{6}$.

(3) High-frequency approximation ($\kappa=\kappa_H$, $\gamma=\gamma_H$). For high frequencies, the higher terms in the sum in Eq. (A4) increase η_I (and therefore the decrement and the quantity γ/κ) over the value given by the first term of the sum by a factor of $\sum_{\omega=0}^{\infty}1(2/u+1)^2=\pi^2/8$. Hence, $\gamma_H/\kappa_H=1$. However, $\bar{\eta}_R$ and therefore the modulus change ϕ are more strongly affected. There are now two high-frequency regions. For $\omega>>3/\tau_F$, the higher-order terms contribute equally to the modulus for $\omega\tau_F<2\mu+1$ and even change the frequency dependence. It has been shown by Wire and Granato[25] that an expression which describes $\bar{\eta}_R$ adequately is given by

$$\bar{\eta}_R=\frac{8}{\pi^4}\frac{L_N^2}{C}b\sigma_0\frac{1}{1+2(\omega\tau_F)^{3/2}}\,. \tag{A8}$$

Since this is not of Debye form, the decrement and modulus can be fitted at only one frequency, and the values of κ_H and γ_H become, therefore, frequency dependent with the values listed in Table I. It should be noticed that the $\omega^{-3/2}$ region develops only after about $\omega\tau_F>5$ so that the modulus is already only a few percent of its maximum value. Since the maximum modulus changes observed are of the order of a few percent, this dependence would be difficult to observe experimentally, and in fact has never been detected.

(4) Zero-order approximation ($\kappa=\kappa_0$ *and* $\gamma=\gamma_0$). Since the zero-order approximation fits the low-frequency modulus (ϕ), one obtains for κ_0 the same value as for the low-frequency approximation, i.e., $\kappa_0=\kappa_L$ [Eq. (A5)]. Since it also fits the high-frequency decrement, which is determined by $\beta=\gamma/\kappa$, one obtains

$$\frac{\gamma_0}{\kappa_0}=\frac{\gamma_H}{\kappa_H}\,,$$

i.e., (A9)

$$\gamma_0=\frac{\kappa_L\gamma_H}{\kappa_H}=1 \text{ and } \kappa_0=\kappa_L=1\,.$$

A more thorough discussion of this approximation is given in Appendix B.

APPENDIX B: THE ZERO-ORDER APPROXIMATION

According to Eq. (A1), the displacement amplitude $\eta(x,\omega)$ of a dislocation is given as a solution of

$$i\omega B_c\eta-C\eta''=b\sigma_0 \tag{B1}$$

for the appropriate boundary conditions. Instead of the complicated true solution $\eta(x,\omega)$ of Eq. (B1), however, simpler (but similar) functions $\eta(x,\omega)$ are often useful which no longer satisfy Eq. (B1) but satisfy simpler equations instead. Thus the functions $\eta_L(x)$ and $\eta_H(\omega)$ can be introduced satisfying the equations

$$-C\eta''_L=b\sigma_0 \tag{B2}$$

and

$$i\omega B_c\eta_H=b\sigma_0\,. \tag{B3}$$

Since these equations follow from Eq. (B1) either for very low or very high frequencies, η_L and η_H are good approximations only in one of the two frequency ranges. For this reason Eq. (B1) will be modified here in such a way that the solution which will be called $\eta_0(x,\omega)$ approximates the true solution $\eta(x,\omega)$ of Eq. (B1) over the whole frequency range.

This is done here by replacing Eq. (B1) by

$$i\omega B_c\bar{\eta}_0 - C\eta_0'' = b\sigma_0 , \tag{B4}$$

where $\bar{\eta}_0$ is again the average displacement. One recognizes the following.

(i) For very low frequencies Eq. (B4) goes over into Eq. (B2) so that in first order, $\eta_0(x)$ gives the correct low-frequency solution of Eq. (B1) and thus the correct low-frequency modulus (i.e., also the correct relaxation strength).

(ii) For very high frequencies Eq. (B4) goes over into Eq. (B3) [since η_H is independent of x, i.e., $\eta_H(x)=\bar{\eta}_H$] so that, in first order, $\eta_0(x)$ gives the correct high-frequency solution of Eq. (1) and thus the correct high-frequency damping.

With the trial solution

$$\eta_0(x,\omega)=f(\omega)\eta_L(x) , \tag{B5}$$

Eq. (B4) leads to

$$i\omega B_c f\bar{\eta}_L + fb\sigma_0 = b\sigma_0 . \tag{B6}$$

Here $\eta_L(x)$ is the solution of Eq. (B2) and $f(\omega)$ is a factor depending on ω but not on x. Inserting $f(\omega)$, which is determined by Eq. (B6), into (B5) gives

$$\eta_0(x,\omega)=\frac{\eta_L(x)}{1+i\omega B_c\bar{\eta}_L/b\sigma_0} . \tag{B7}$$

By averaging over x, one indeed obtains $\bar{\eta}_0=\bar{\eta}_L$ for low frequencies and $\eta_0=b\sigma_0/i\omega B$ for high frequencies. From $\eta_0(\omega)$, with Eqs. (2), (3), and (5), the expressions for relaxation strength Δ and time τ are found. For the boundary condition $y(0)=y(L)=0$, Eq. (B2) gives [cf. Eqs. (A6) and (A7)]

$$\eta^L(x)=\frac{b\sigma_0 L^2}{2C}\frac{x}{L_N}\left[1-\frac{x}{L_N}\right] , \quad \bar{\eta}_L=\frac{b\sigma_0 L_N^2}{12C} \tag{B8}$$

Introducing this in Eq. (B7) then leads directly to the relaxation strength and time given by Eqs. (5) with $\kappa=1$ (as for the low-frequency approximation) and $\gamma=1$ (so that the high-frequency approximation value $\gamma/\kappa=1$ is preserved).

It is to be noted that this is a simple Debye form, whereas a much more complicated expression would result using the correct differential equation (B1). The advantage of the first-order approximation is then that we have obtained a simple Debye-form approximation, which has the correct first-order features of the response, while not having had to solve the whole differential equation (B1), but only the simple case for $\omega B_C=0$.

One can try to find solutions of Eq. (B1) by perturbation calculations. For the low-frequency range the first term is small compared to the second one so that as a zero-order approximation $\eta_0(x)=\eta_L(x)$ is obtained. By introducing $\eta=\eta_0+\eta_1=\eta_L+\eta_1$ with $\eta_1<<\eta_L$ and simple integration, the first-order approximation η_1 can be found, which gives the expression for the damping. The resulting factors κ and γ come out to be the same as the ones given in Appendix A for the low-frequency approximation.

In the high-frequency range the second term is small and $\eta_0=\eta_H$ is the zero-order approximation. In this case, however, the introduction $\eta=\eta_H+\eta_1$ with $\eta_1<<\eta_H$ does not lead to a second-order approximation and to an expression for the modulus if the drag is continuous ($n=\infty$). The high-frequency perturbation calculation also works only for the case of finite n (cf. Appendix C).

Another way of simplifying Eq. (B1) is to consider only average values and to replace Eq. (B1) by

$$i\omega B_C\bar{\eta}_A - \bar{C}\eta_{Axx} = b\sigma_0 . \tag{B9}$$

Here, however, any function $\eta_A(x)$ satisfying the boundary conditions also satisfies Eq. (B9) so that choosing the displacement function $\eta_A(x)$ becomes a question of intelligent guessing. By trying $\eta^A=A\sin\pi(x/L)$ the values $\kappa=\pi^2/12$, $\gamma=\pi^2/12$ are obtained, while for a triangle-shaped displacement function, $\kappa=\frac{2}{3}$ and $\gamma=\frac{2}{3}$. This will always give the correct high-frequency decrement but will only give the correct low-frequency modulus when the correct low-frequency displacement function has been chosen. In the latter case, this becomes the zero-order approximation.

APPENDIX C: RELAXATION EFFECTS CAUSED BY DISCRETE DRAG

We consider a dislocation of length L_N with $p=n-1$ equidistant pinning points separated by a

distance $L_d = L_N/n$ as in Fig. 2, with each pinner having the mobility $m = D/kT$. The continuous dragging force B_c acting between the pinners and all inertia effects are neglected. Then, each pinning point experiences two types of forces [Fig. 2(c)].

(i) A force due to the adjacent pinning points occurs if these have a different displacement than the pinning point under consideration. It is represented by the vertical component of the line tension of the in between dislocation segments for an external stress $\sigma = 0$ when these segments are straight and form a polygon-shaped dislocation line. The force acting upon the pinning point is then given by

$$F_\nu = C(\sin y_{\nu+1} - \sin y_\nu) \approx \frac{C}{L_d}(y_{\nu-1} - 2y_\nu + y_{\nu+1}) \quad \text{(C1)}$$

with y being the displacement of the νth pinning point.

(ii) The force due to the external stress $\sigma = \sigma_0 \exp(i\omega t)$, which is given by

$$F_\sigma = bL_d\sigma = bL_d\sigma_0 \exp(i\omega t) . \quad \text{(C2)}$$

This force is transferred to the pinning points by the additional bowing out of the in between loops which is completely in phase with the external stress, since these loops are assumed to have no drag acting upon them. The velocity of the νth pinning point is then given by $\dot{y}_\nu = m(F_\nu + F_\sigma)$ or, with $B_d = 1/mL_d$ [Eq. (8)] by

$$B_d\dot{y}_\nu - \frac{C}{L_d^2}(y_{\nu-1} - 2y_\nu + y_{\nu+1}) = b\sigma_0 \exp(i\omega t) . \quad \text{(C3)}$$

With $y_0 = y_n = 0$ this is a set of $n-1$ equations corresponding to the equation of motion [Eq. (1)] in the continuous case. With $y_\nu = \eta_\nu \exp(i\omega t)$ the form

$$i\omega B_d\eta_\nu - \frac{C}{L_d^2}(\eta_{\nu-1} - 2\eta_\nu + \eta_{\nu+1}) = b\sigma_0 \quad \text{(C4)}$$

corresponding to Eq. (A1) is obtained. After solving for the different η_ν, the average displacement

$$\bar{\eta} = \frac{1}{n}\sum_{\nu=1}^{n}\eta_\nu \quad \text{(C5)}$$

represents the area of the polygon of Fig. 2(c). Finally, by introducing the real and imaginary part of $\bar{\eta}$ into Eq. (2) the modulus change and decrement are obtained.

Exact solution. The displacement η_ν may be developed in a finite Fourier series. It is also necessary to express $b\sigma_0$ in terms of its Fourier components:

$$\eta_\nu = \sum_{\mu=0}^{n-1} a_{2\mu+1}^{(n)} \sin\nu(2\mu+1)\pi/n , \quad \text{(C6)}$$

$$b\sigma_0 = b\sigma_0 \sum_{\mu=0}^{n/2-1} b_{2\mu+1}^{(n)} \sin\nu(2\mu+1)\pi/n . \quad \text{(C7)}$$

The expansion coefficients $b_{2\mu+1}^{(n)}$ are given as the ratio of two determinants

$$b_{2\mu+1}^{(n)} = \frac{\det \sin[\nu(2m'+1)\pi/n]}{\det \sin[\nu(2m+1)\pi/n]} , \quad \text{(C8)}$$

where

$$\mu = 0,1,2,\ldots,\frac{n}{2}-1 ,$$

$$\nu = 1,2,\ldots,\frac{n}{2} ,$$

$$m = 0,1,\ldots,\frac{n}{2}-1 ,$$

and

$$2m'+1 = \begin{cases} 2m+1 , & m \neq \mu \\ n/2 , & m = \mu , \end{cases}$$

and the rows and columns of the determinant are given by ν and m or m', respectively. The first few coefficients are

$$b_1^{(2)} = 1 \quad (\mu = 0) ,$$

$$b_1^{(3)} = 2/\sqrt{3} \quad (\mu = 0) ,$$

$$b_2^{(4)} = \frac{2+\sqrt{2}}{2\sqrt{2}} , \quad b_3^{(4)} = \frac{2-\sqrt{2}}{2\sqrt{2}} \quad (\mu = 0,1) ,$$

$$b_1^{(6)} = \frac{2}{3\sqrt{3}}(1+\sqrt{3}) , \quad b_3^{(6)} = \frac{2}{3\sqrt{3}}(\sqrt{3}/2) ,$$

$$b_5^{(6)} = \frac{2}{3\sqrt{3}}(-\tfrac{3}{2}+\sqrt{3}) \quad (\mu = 0,1,2) ,$$

$$b_{2\mu+1}^{(n)} \underset{n>>1}{\rightarrow} \frac{1}{2\mu+1} .$$

Substituting Eqs. (C6) and (C7) into (C4) determines the expansion coefficients as

$$a_{2\mu+1}^{(n)}=\frac{b\sigma_0 L_N^2}{4C}\frac{b_{2\mu+1}^{(n)}}{n^2\sin[(2\mu+1)\pi/2n]+i\omega BL_N^2/4c} . \tag{C9}$$

Then, taking the average over all pinning-point positions [Eqs. (C5)], one obtains

$$\bar{\eta}(n)=\sum_{\mu=0}^{n/2-1} a_{2\mu+1}^{(n)}\frac{1}{n}\cot[(2\mu+1)\pi/2_n)] \tag{C10}$$

and

$$\bar{\eta}(n)=\sum_{\mu=0}^{n/2-1}\frac{(b\sigma_0 L_N^2/4C)(1/n)\cot[(2\mu+1)\pi/2n]b_{2\mu+1}^{(n)}}{[n^2\sin^2(2\mu+1)\pi/2n+i\omega BL_N^2/4c]} . \tag{C11}$$

(1) First-term Fourier approximation [$\gamma=\gamma_F(n)$, $\kappa=\kappa_F(n)$]. This is obtained by using only the first term of Eq. (C11), as in the continuous drag case.

(2) Low-frequency approximation [$\kappa=\kappa_L(n)$, $\gamma=\gamma_L(n)$]. For low frequencies again a perturbation calculation (compare with Appendix B) will be made. With $\eta_\nu=\eta_\nu^{(0)}+\eta_\nu^{(1)}$ one obtains the equations

$$-\frac{C}{L_d^2}(\eta_{\nu-1}^{(0)}-2\eta_\nu^{(0)}+\eta_{\nu+1}^{(0)})=b\sigma_0 ,$$

$$\frac{C}{L_d^2}(\eta_{\nu-1}^{(1)}-2\eta_0^{(1)}+\eta_{\nu+1}^{(1)})=i\omega Bd , \tag{C12}$$

which are solved by the expressions

$$\eta_\nu^{(0)}=\frac{b\sigma_0 L_d^2}{2C}\nu(n-\nu) ,$$

$$\eta_\nu^{(1)}=\frac{-i\omega B_d b\sigma_0 L_d^4}{24C^2}\times[(n^2+1)\nu(n-\nu)+\nu^2(n-\nu)^2] . \tag{C13}$$

The average values according to Eq. (C5) are

$$\bar{\eta}^{(0)}=\frac{b\sigma_0 L_d^2}{12C}(n^2-1) ,$$

$$\bar{\eta}^{(1)}=\frac{-i\omega B_d b\sigma_0 L_d^4}{120C^2}(n^4-1) , \tag{C14}$$

which, introduced into Eq. (2), lead to the $\gamma_L(n)$ and $\kappa_L(n)$ values listed in Table I.

(3) High-frequency approximation [$\gamma=\gamma_H(n)$, $\kappa=\kappa_H(n)$]. A perturbation calculation can be applied to Eq. (C4), leading to

$$\eta_\nu+i\epsilon(\nu_{\nu+1}-2\eta_\nu+\eta_{\nu-1})=ib\sigma_0/\omega B_b , \tag{C15}$$

where the expansion parameter is given by

$$\epsilon=c/\omega B_d L_d^2=n^2 c/\omega B_d L_N^2 . \tag{C16}$$

Then, with

$$\eta_\nu(\epsilon)=\eta_\nu^{(0)}+\epsilon\eta_\nu^{(1)}+\cdots , \tag{C17}$$

one obtains

$$\eta_\nu^{(0)}=-ib\sigma_0/\omega B_d , \quad \nu=1,2,\ldots,n-1 \tag{C18}$$

$$\eta_\nu^{(1)}=i(\eta_{\nu+1}^{(0)}-2\eta_\nu^{(0)}+\eta_{\nu-1}^{(0)}) \tag{C19}$$

$$=\begin{cases} b\sigma_0/\omega B_d , & \nu=1,n-1 \\ 0 \text{ otherwise} . \end{cases}$$

Thus, the zero-order displacement gives the decrement and is the same for all pinners, while the first-order correction giving the modulus is nonzero only for the movable pinners adjoining the strong pinning points. Then using Eq. (C5), one finds

$$\bar{\eta}=b\sigma_0\left[\frac{2nC}{\omega^2 B_d^2 L_N^2}-i\frac{n-1}{n}\frac{1}{\omega B_d}\right] . \tag{C20}$$

Equation (C20) leads, with Eq. (2), to the values of $\kappa_H(n)$ and $\gamma_H(n)$ listed in Table I. One sees from Eq. (C16), that for fixed frequency, the condition $\epsilon<1$ will eventually be exceeded as n increases and this approximation will then no longer be valid. When this occurs, the behavior is closely described by the high-frequency string limit described in Appendix A. There are thus three high-frequency ranges. For frequencies just above the maximum of the decrement when only the first normal mode

of the string is excited, the first-term Fourier approximation is valid. The "high-frequency" limit can be described approximately by $\omega\tau_F(n) \geq \omega B(n) L_N^2/\pi^2 c = n^2/4$. The "high-frequency string limit" is then given approximately by $4 \leq \omega\tau_F(n) \leq n^2/4$. Whether measurements are begun at frequencies greater or lower than $1/\tau_F$, one always eventually moves into the high-frequency string limit as n grows indefinitely. For $n=2$ and 3, there exists no high-frequency string limit since for these cases there is only one term in the Fourier series, and the Debye representation of the response is therefore exact for all frequency ranges.

For high frequencies, the modulus defect ϕ_H is proportional to $(\Lambda/B_d^2 L_N^2)(\gamma^2/\kappa)$ [Eqs. (3) and (5)]. At high frequencies, the only part of the displacement that is in phase with the applied stress is that part close to the firm pinning points since the velocity there is low. The modulus change must, therefore, be proportional to the number of firm pinning points as a function of n, i.e., $\phi_H \propto \Lambda/L_N$. But $n = L_N/L_d$ and can be varied either by changing L_d or L_N. Since for large n, γ_H/κ_H becomes independent of n (see Sec. IV), one has $\phi_H \propto \Lambda\gamma_H^2/B^2 L_N^2 \kappa_H$ or $\phi_H \propto \Lambda\gamma_H/L_N^2$ for fixed L_d (and therefore B_d). Thus γ_H must increase linearly in L_N or n. This is the dependence given in Table I for large but finite n ($\omega B L_N^2/C >> n^2$). For the limit of $n \to \infty$, the string equation is valid, and this contains n only implicitly through the dependence of B_d and L_N on n. The only function of $\omega\tau_F = \omega B_d L_N^2/\pi^2 C$ which is then linear in n or L for fixed L_d is $\sqrt{\omega\tau_F}$.

(4) Zero-order approximation. Again $\kappa_0(n) = \kappa_L(n)$ and $\gamma_0(n)/\kappa_0(n) = \gamma_H^{(n)}/\kappa_H^{(n)}$ by the definition of the first-order approximation (cf. Appendix A).

---

*Permanent address.

[1]A. V. Granato and K. Lücke, J. Appl. Phys. 27, 582 (1956).

[2]J. S. Koehler, in *Imperfections in Nearly Perfect Crystals,* edited by W. Shockley *et al.* (Wiley, New York, 1952), p. 197.

[3]G. Leibfried, Z. Phys. 127, 344 (1950).

[4]A. Brailsford, in *Internal Friction and Ultrasonic Attenuation in Crystalline Solids,* edited by D. Lenz and K. Lücke (Springer, New York, 1975), Vol. II, p. 1.

[5]A. V. Granato, in *Internal Friction and Ultrasonic Attenuation in Crystalline Solids,* Ref. 4, p. 33.

[6]J. O. Kessler, Phys. Rev. 106, 646 (1957).

[7]J. Weertmann, J. Appl. Phys. 28, 193 (1957).

[8]A. H. Cottrell, *Dislocations and Plastic Flow in Crystals* (Clarendon, Oxford, 1953), p. 138.

[9]R. Kamel, Acta Metall. 9, 65 (1961).

[10]G. Schoeck, in *Proceedings of the International Conference on Crystal Defects, Tokyo, 1962* [J. Phys. Soc. Jpn. 18, Suppl. I (1963)]. See also Acta Metall. 6, 617 (1963).

[11]P. Schiller, Phys. Status Solidi 5, 391 (1964).

[12]A. A. Blistanov and M. P. Shaskol'skaya, Fiz. Tverd. Tela (Leningrad) 6, 735 (1964) [Sov. Phys.—Solid State 6, 573 (1964)].

[13]K. Yamafuji and C. L. Bauer, J. Appl. Phys. 36, 3288 (1965)

[14]K. Lücke and J. Schlipf, in *The Interactions between Dislocations and Point Defects,* edited by B. L. Eyre (AERE, Harwell, 1968), Vol. 1, p. 118.

[15]W. Winkler-Gniewek, thesis, Technische Hochschule Aachen, 1973 (unpublished); J. Schlipf, W. Winkler-Gniewek, and R. Schindlmayr (unpublished).

[16]H. M. Simpson and A. Sosin, Phys. Rev. B 5, 1382 (1972); H. M. Simpson, A. Sosin, R. G. Edwards, and S. L. Seiffert, Phys. Rev. Lett. 26, 897 (1971); H. M. Simpson and A. Sosin, Phys. Rev. B 16, 1489 (1977).

[17]A. Sosin, in *Internal Friction and Ultrasonic Attenuation in Crystalline Solids,* Ref. 4, p. 109.

[18]T. O. Ogurtani, Phys. Rev. B 21, 4373 (1980).

[19]J. Garber and A. V. Granato, in *Fundamental Aspects of Dislocation Theory,* edited by J. A. Simmons *et al.* [Natl. Bur. Stand. (U.S.) Spec. Publ. 317, I, 419 (1970)]. See also J. Phys. Chem. Solids 31, 1863 (1970).

[20]A. Hikata and C. Elbaum, in *Internal Friction and Ultrasonic Attenuation in Crystalline Solids,* Ref. 4, p. 188.

[21]A. Seeger and P. Schiller, in *Physical Acoustics,* edited by W. P. Mason (Academic, New York, 1966), Vol. 3A, p. 361.

[22]T. Suzuki and C. Elbaum, J. Appl. Phys. 35, 1539 (1964).

[23]D. Lenz and K. Lücke, in *Internal Friction and Ultrasonic Attenuation in Crystalline Solids,* Ref. 4, p. 48.

[24]A. V. Granato, in *Fundamental Aspects of Radiation Damage in Metals,* edited by M. T. Robinson and F. W. Young, Jr., National Technical Information Service (U.S. Department of Commerce, Springfield, Virginia, 1975).

[25]G. Wire, thesis, University of Illinois, 1972 (unpublished); G. Wire and A. V. Granato (unpublished).